Electronic Supplementary Information

Dendronized Delayed Fluorescence Emitters for Non-Doped, Solution-Processable Organic Light-Emitting Diodes with High Efficiency and Low Efficiency Roll-Off Simultaneously: Two Parallel Emissive Channels

Yifan Li, † Guohua Xie, † Shaolong Gong, Kailong Wu, and Chuluo Yang*

Hubei Collaborative Innovation Center for Advanced Organic Chemical Materials, Hubei Key Lab on Organic and Polymeric Optoelectronic Materials, Department of Chemistry, Wuhan University, Wuhan, 430072, People's Republic of China

Table S1. Thermal, photophysical, and electrochemical data of the materials

Compound	$T_d/T_g/T_m$ [°C]	λ_{abs} [nm][a]	λ_{ems} [nm][a]	FWHM [nm]	Φ_{PL} [%][b]	HOMO/LUMO [eV][cd]	S_1 [eV]	ΔE_{ST} [eV]
CDE1	471/283/313	289,299,349	520	91	77	-5.12/-2.54	2.69	0.11
CDE2	507/289/367	289,298,348	499	89	75	-5.25/-2.69	2.84	0.15

[a] Measured in the film; [b] Fluorescence quantum yields in solid state films, measured on the quartz plate using an integrating sphere; [c] Determined from the onset of oxidation potentials; [d] Deduced from HOMO and E_g estimated from the red edge of the longest absorption wavelength for the solid-film sample.

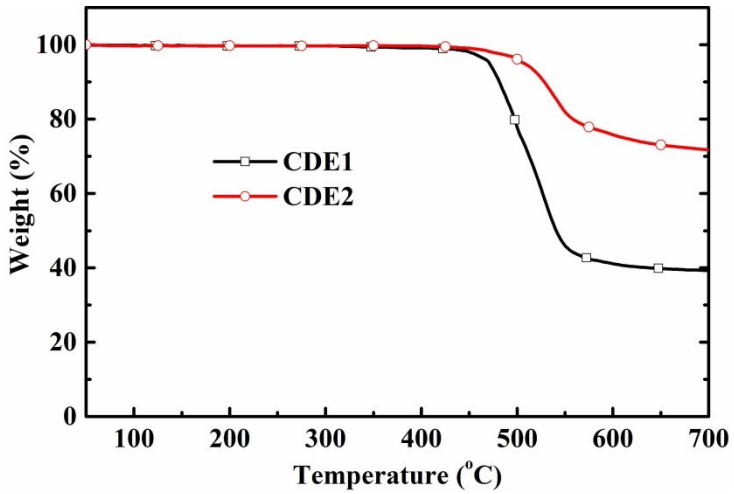

Fig. S1. TGA traces of CDE1 and CDE2

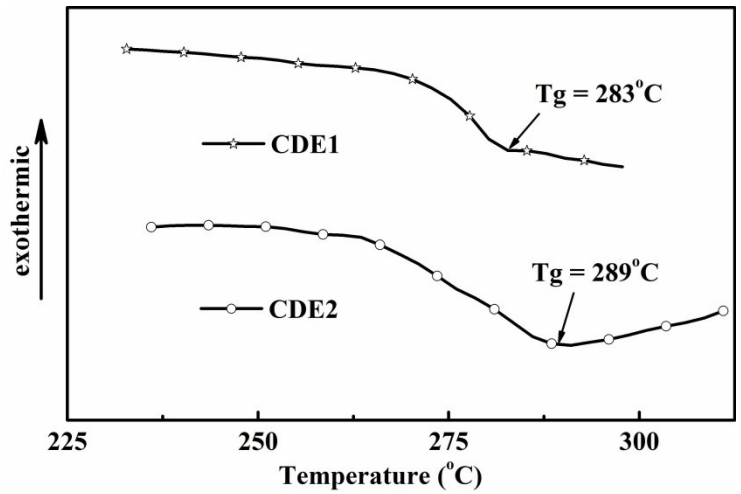

Fig. S2. DSC curves of CDE1 and CDE2 measured at a heating rate of 10 °C min^{-1} under N_2.

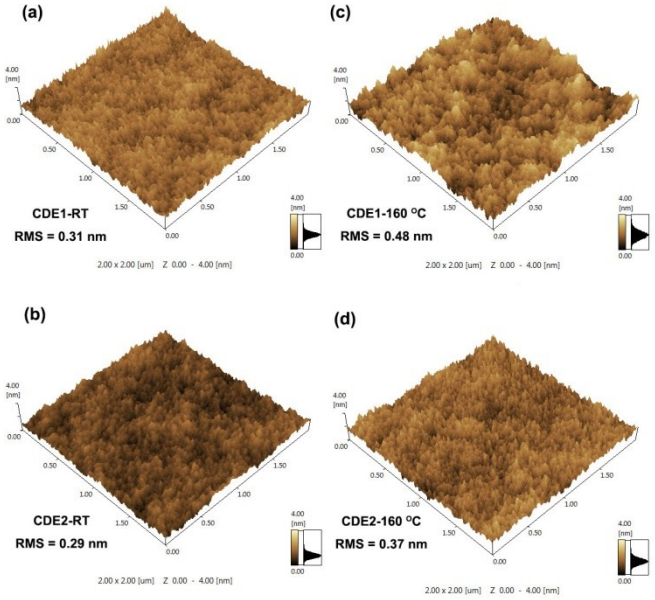

Fig. S3. 3D AFM topographic images of the as-cast films of CDE1 (a) and CDE2 (b), and the annealed films at 160 °C of CDE1 (c) and CDE2 (d).

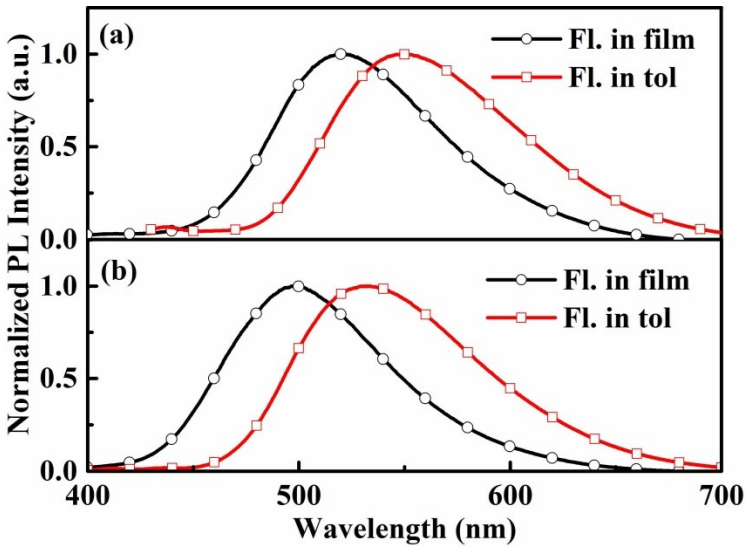

Fig. S4. The fluorescence spectra of CDE1 (a) and CDE2 (b) in film and toluene (1×10^{-5} M).

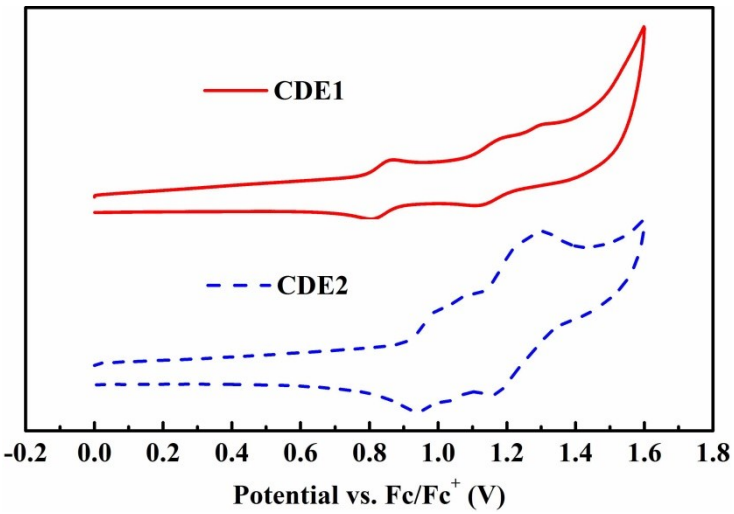

Fig. S5. Cyclic voltammograms of the materials in CH_2Cl_2 for oxidation.

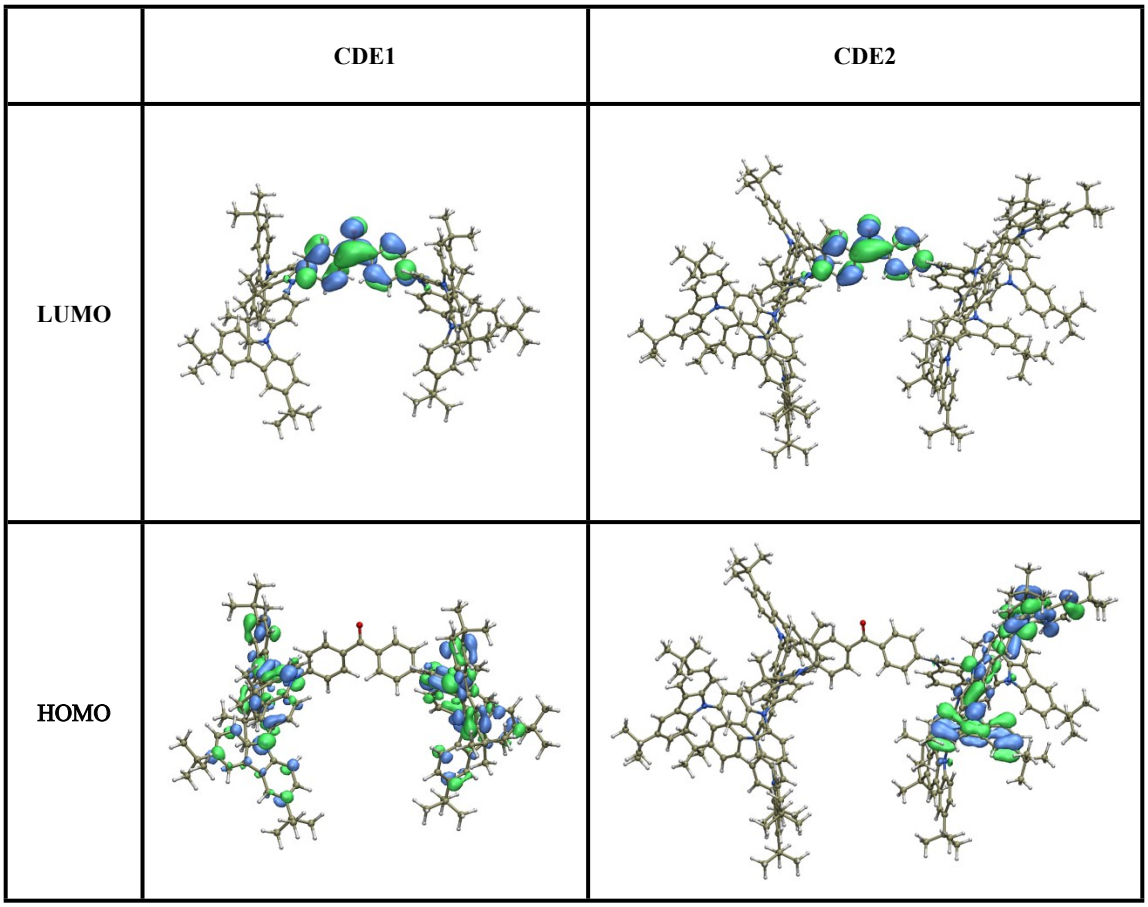

Fig. S6. HOMO and LUMO distributions in the two dendrimers calculated at the b3lyp/6-31G(d) level of theory.

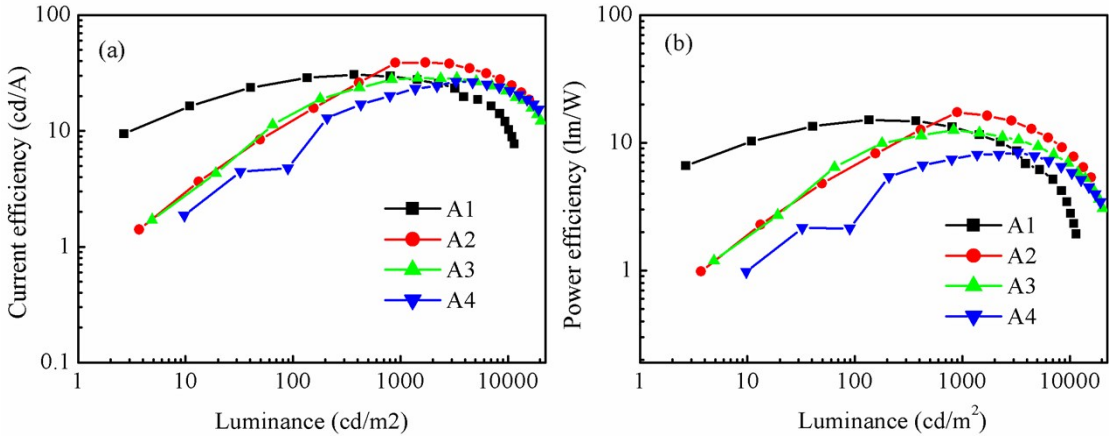

Fig. S7. (a) Current efficiency versus luminance curves, and (b) power efficiency versus luminance curves for Devices A1-A4.

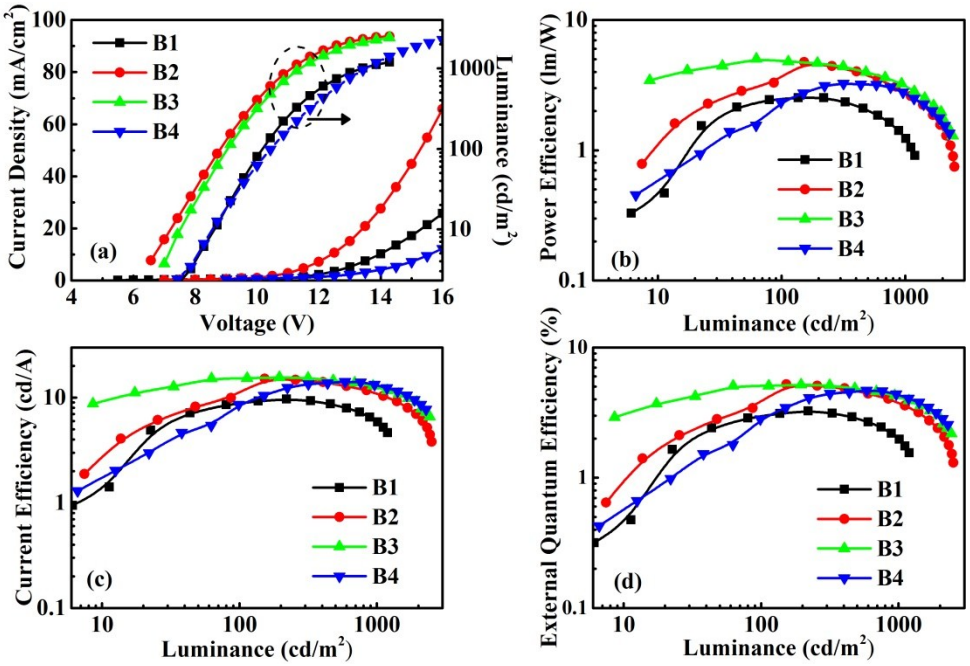

Fig. S8. (a) Current density−voltage−luminance (*J*−*V*−*L*) characteristics, (b) power efficiency versus luminance curves, (c) current efficiency versus luminance curves, and (d) external quantum efficiency versus luminance curves for Devices B1-B4.

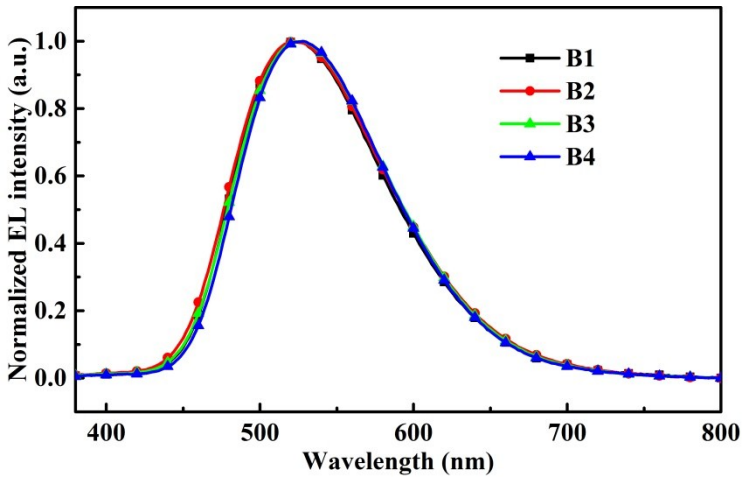

Fig. S9. Normalized EL spectra of Devices B1-B4.

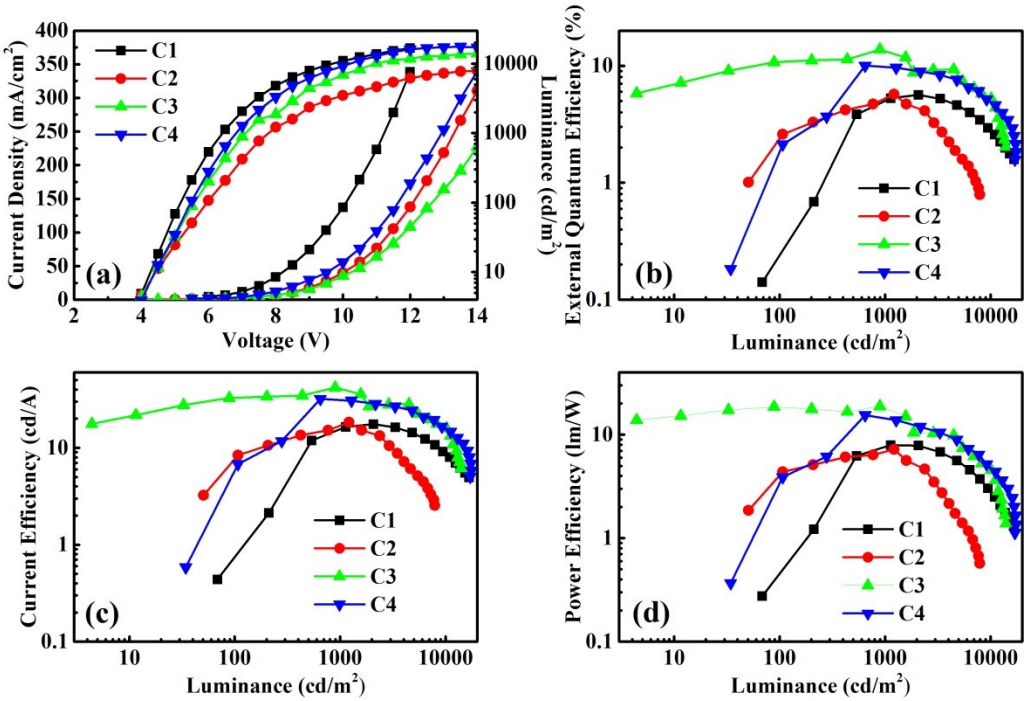

Fig. S10. (a) Current density−voltage−luminance (*J*−*V*−*L*) characteristics, (b) external quantum efficiency versus luminance curves, (c) current efficiency versus luminance curves, and (d) power efficiency versus luminance curves for Devices C1-C4.

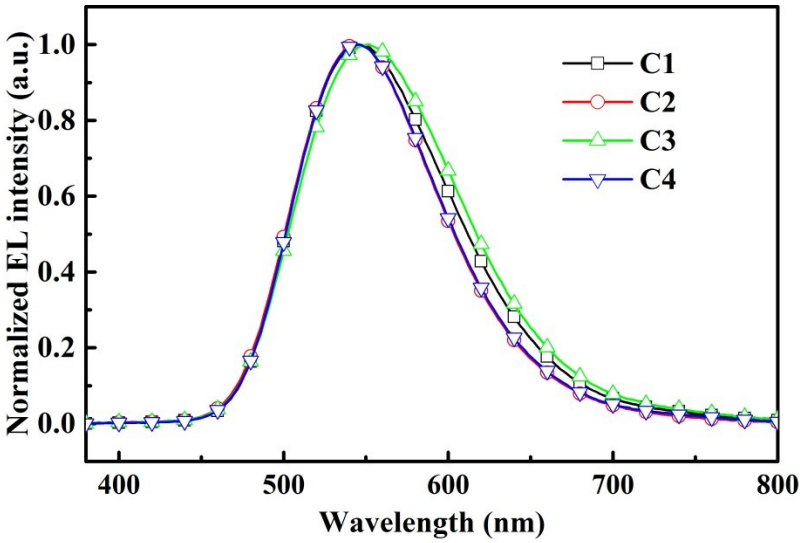

Fig. S11. Normalized EL spectra of Devices C1-C4.

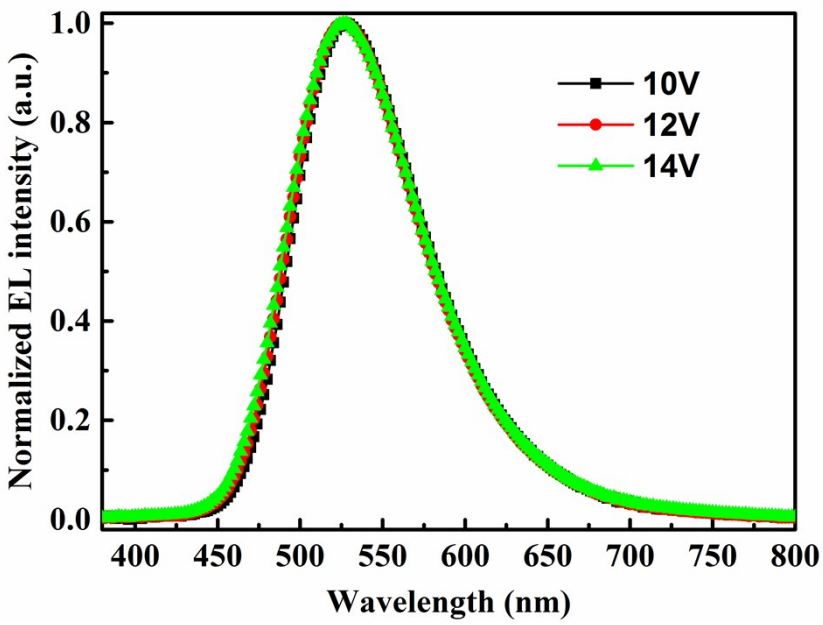

Fig. S12. Normalized EL spectra of the single layer device of ITO/PEDOT:PSS/CDE1/Ca/Al.

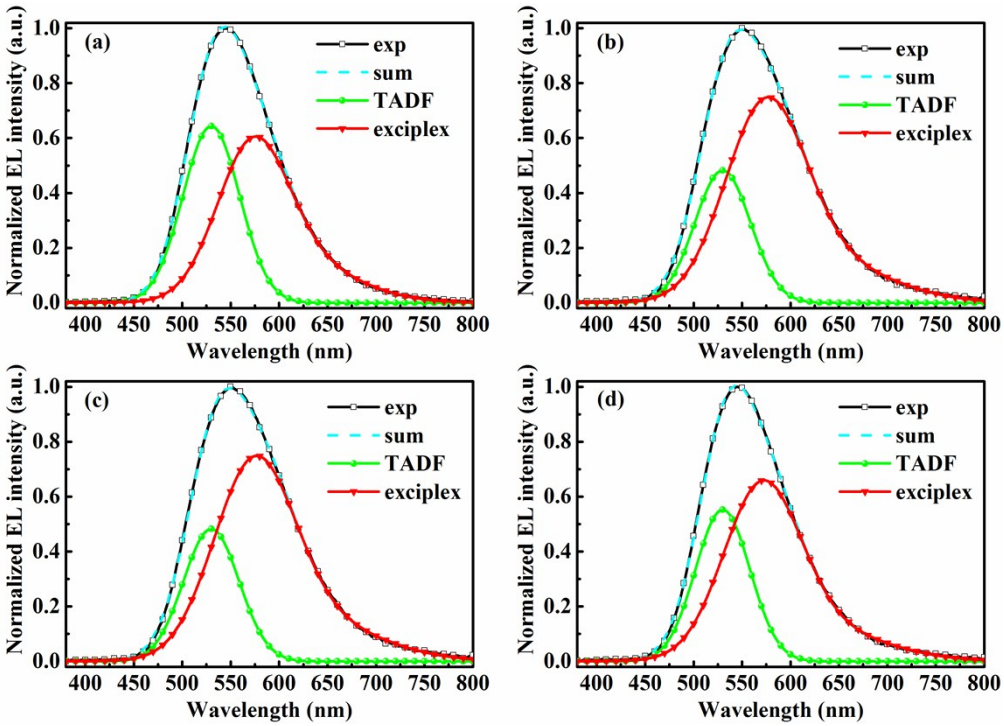

Fig. S13. Normalized EL spectra via Gaussian fitting of Devices C1 (a), C2 (b), C3 (c) and C4 (d).

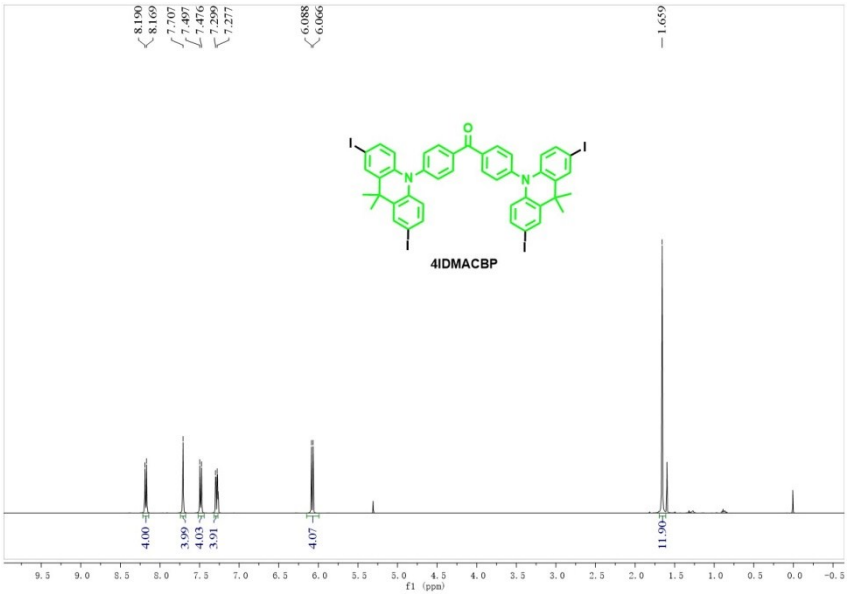

Fig. S14. [1]H NMR spectrum of **4IDMACBP**.

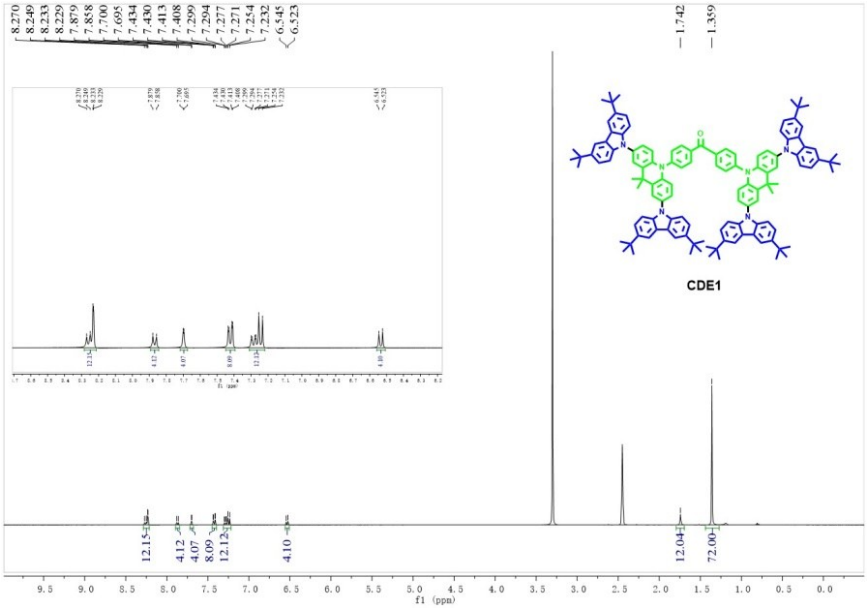

Fig. S15. [1]H NMR spectrum of **CDE1**.

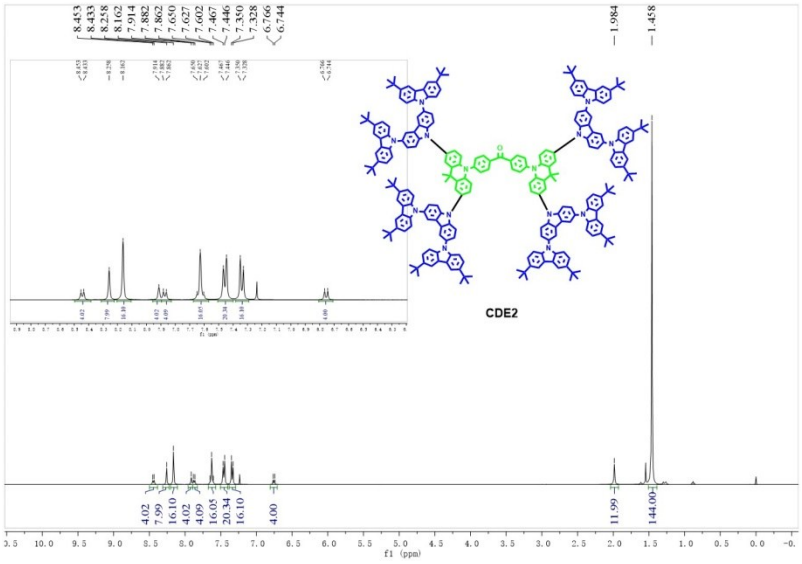

Fig. S16. ^{1}H NMR spectrum of **CDE2**.